1 Supplementary explanatory material

1.1 Section 3.1, before Proposition 1

1.1.1 Radical difference with 'the jump occurred at T_{i+k} is a descendant'

Remark 1. The event 'the next jump belongs to the previous cluster' is radically different from the event 'the occurred jump is a descendant'. First of all, in the former case the jump time T_{i+k} is unknown, while in the latter the jump time is known. Secondly, the probability of the former event coincides with the probability that the intensity at the random time T_{i+k} is greater than $\lambda_0(1+\epsilon)$; while the probability that a jump observed at t is a descendant is given by the ratio $q \doteq \frac{\lambda_t - \lambda_0}{\lambda_t}$ (see Zhuang et al., 2002). The method proposed in this paper allows us to obtain a more precise measure than q of how long an agglomeration of jumps triggered by a specific event is going to last. For example, within the simulation exercise in Section 5, where $\bar{s}$ is not a jump time, the estimated $P\{T_{i+k} < \bar{s} + t_\epsilon(\bar{s})\}$ for GE is above 90% (which turns out to be close to the bounds given in Proposition 1). On the contrary, if we replace $\lambda_{T_{i+k}}$ with $\lambda_{\bar{s}}$ we would obtain $q = 0.51$.

1.2 Stochastic increasingness: Section 3.2

1.2.1 Consequence of Proposition 2.

Corollary 1. *$T_{n+1} - T_n$ is stochastically decreasing in λ_{T_n}.*

Proof. From (11), by differentiating the expression $P\{T_{n+1} - T_n > \tau | \bar{\lambda}_{T_n} = \ell\}$ wrt ℓ, we reach

$$\frac{d}{d\ell} P\{T_{n+1} - T_n > \tau | \bar{\lambda}_{T_n} = \ell\} = \frac{1}{\beta}(e^{-\tau\beta} - 1) \exp\left(e^{-\tau\beta}(\ell - \lambda_0 + \alpha) - \beta\lambda_0\tau - \ell - \alpha + \lambda_0\right),$$

which is negative $\forall \tau > 0$. □

Intuitively, the result means that, if the value $\ell = \lambda_{T_n}$ of the jump intensity immediately before a jump time T_n is large, then also the value $\lambda_{T_n+} = \lambda_{T_n} + \alpha$ of the jump intensity just after T_n is large, thus the probability of the occurrence of a jump in the near future is high, and one expects that the jump time T_{n+1} is close to T_n, i.e. $T_{n+1} - T_n$ is small.

1.3 Remark on Section 4

Remark 2. [About Theorem 3] If we only rely on discrete observation and want to implement the recursion, then we can write eq. (14) in a more suitable form. Let us indicate by $\mathcal{I}_n$ any interval containing $\tilde{\lambda}_n$. Then, by Theorem 3 we have:

$$\mathcal{I}_n = \left[1 - (1 - \inf \mathcal{I}_{n-1})^{e^{-\beta\delta}} \exp\left((e^{-\beta\delta} - 1)\left(\delta\lambda_0 + \omega_{n-1}\frac{\alpha e^{-\beta\delta}}{\beta}\right)\right), \quad (1)$$

$$1 - (1 - \sup \mathcal{I}_{n-1})^{e^{-\beta\delta}} \exp\left((e^{-\beta\delta} - 1)\left(\delta\lambda_0 + \omega_{n-1}\frac{\alpha}{\beta}\right)\right)\right). \quad (2)$$

The case when $\tilde{\lambda}_{n-1}$ is given corresponds to $\mathcal{I}_{n-1} = \{\tilde{\lambda}_{n-1}\}$, so that $\inf \mathcal{I}_{n-1} = \sup \mathcal{I}_{n-1} = \tilde{\lambda}_{n-1}$.

1.4 Empirical application, Section 5

1.4.1 Identification of the jumps

When $(\Delta_i X)^2 > r_i(\delta)$ then the *standardized return* $\frac{\Delta_i X}{\hat{\sigma}_{t_i}\sqrt{\delta}}$ has an absolute value that is larger than the theoretical level $\sqrt{2\log\frac{1}{\delta}}$, which makes it incompatible with the increment of a Brownian semimartingale, even if the spot volatility σ_{t_i} was high. The threshold $r_i(\delta)$ has been shown (Figueroa-López and Mancini, 2019) to be optimal in minimizing both the Mean Squared Error and the Conditional Mean Squared Error when estimating the integrated variance $IV = \int_0^T \sigma_s^2 ds$ by the Truncated Realized Variance $\hat{IV} = \sum_{i=1}^m (\Delta_i X)^2 \mathbf{1}_{\{(\Delta_i X)^2 \le r_i(\delta)\}}$ in a framework where the jumps in X have finite activity and the volatility σ is constant. However the optimality result is being extended to the more general case of volatility process with càdlàg paths. Further, in the mentioned paper a simulation study shows that using $r_i(\delta)$ also spot σ is correctly estimated, even in the presence of leverage between σ and W.

We estimate spot sigma and the jump times recursively and taking into account the typical U-shape diurnal effect of spot volatility. First we implemented the procedure described in Bollerslev and Todorov, 2011, Appendix B, to estimate the volatility *time of day* effect (TOD). TOD is a factor to be multiplied with an estimate of the daily average squared volatility $\left(\sigma^{(a)}_{day}\right)^2$. The factor turns out to display a U shape during the day, i.e. it assumes values around 1.9 at the beginning of the trading day, a minimum of about 0.4 at lunch time and around 0.6 at the end of the day. A realistic estimate of the volatility at time t_j of day ℓ is given by $\sqrt{TOD(t_j)} \cdot \hat{\sigma}^{(a)}_{day\,\ell}$. Each day the average volatility usually changes, while the estimate of the TOD effect at time t_j is the same every day.
Second, we pre-truncate the asset returns taking $\Delta_i X \mathbf{1}_{\{|\Delta_i X| \le 6\bar{\alpha}\sqrt{2\delta\log\frac{1}{\delta}}\}}$, where $\bar{\alpha}$ is calculated within the procedure to obtain TOD, and is an estimate of the average spot sigma within a day, based on the average across all sample days of the daily Bipower Variation. We then apply to the pre-truncated returns a kernel estimator to obtain the average spot volatility during a day. The kernel is a unilateral indicator function and the bandwidth is such that only the observations within a day are used to compute the average volatility for that day.
Third, a first-round threshold for observation j of day ℓ is constructed as

$$r^{(1)}_{j,\ell} = 2\sqrt{TOD_{t_j}} \cdot \hat{\sigma}^{(a,1)}_{day\,\ell} \cdot \delta \log\frac{1}{\delta},$$

and a jump time is identified if $|\Delta_j X| > r^{(1)}_{j,\ell}$.
At this point spot sigma is re-estimated only using the returns in absolute value below the respective $r^{(1)}_{j,\ell}$, in the same way as above (one sided kernel estimator), a second-round threshold is constructed as $r^{(2)}_{j,\ell} = 2\sqrt{TOD_{t_j}} \cdot \hat{\sigma}^{(a,2)}_{day\,\ell} \cdot \delta \log\frac{1}{\delta}$, and new jump times are identified when $|\Delta_j X| > r^{(2)}_{j,\ell}$. Similarly a third round is implemented, and all the found jumps are collected together.

1.4.2 On the independence assumption of λ and σ.

The assumption that N is independent of the other components a, σ, W of the model is consistent with many papers in the literature. Besides Aït-Sahalia et al. (2015), for instance in Duffie et al. (2000) the model with which the empirical application is done in Sec. 4 has constant jump intensity Λ^Q under the risk neutral probability Q. The made assumptions imply that also under the objective probability P the intensity Λ^P turns out to be constant.[1]
Another strand of literature instead assumes that λ can be an affine function of spot σ. As mentioned in Section 5.1, we also considered for our estimated jump times $\hat{T}_i$ a point process having the alternative $\check{\lambda}_t = d + b\sigma_t$. To approximate λ_t we used $\frac{\sum_{t_i \text{within day } t} \Delta_i N}{77\delta}$, and for the spot volatility we used the average daily $\hat{\sigma}_t$ obtained following the non-parametric procedure described in Sec. 5. We checked this model for the selected 20 assets, and we found positive and significant MLE $\hat{d}, \hat{b}$ only for BAC, BHP and GE. However the QQ-plot of the values $\int_{\hat{T}_{i-1}}^{\hat{T}_i} \hat{\check{\lambda}}_t dt$ against values of independent exponential rvs, with parameter 1, turned out to be worse than the one of the values $\int_{\hat{T}_{i-1}}^{\hat{T}_i} \hat{\lambda}_t dt$, where $\hat{\lambda}_t$ is the estimated jump intensity under the Hawkes model.

1.4.3 Estimation of the Exponential Hawkes parameters

The constraints. We impose $\lambda_0, \alpha, \beta > 0$ and $\alpha < \beta$. If it was $\lambda_0 = 0$ we would have no father jumps, so no descendants could be generated, and no jumps at all would occur. If it was $\Phi(0) = \alpha = 0$ then $\Phi \equiv 0$ and N would be a Poisson process.
When $\alpha > 0$, the condition $\beta > 0$ is necessary for the existence of a finite asymptotic stationary measure for λ_t, when $t \to +\infty$. In fact, if $\alpha > 0$, then the effect of the occurrence of any single jump of N is to increase λ instantaneously by α, but then such an effect decays exponentially with speed β, which pushes λ to return back towards the level λ_0. If it was $\beta = 0$ then at any jump of N, the increase by α of λ would not decay, it would be a permanent effect, ending up with explosion of λ for $t \to +\infty$, and in fact the stationarity condition $\int_0^{+\infty} \Phi(x)dx < 1$ would not be satisfied.
Finally, given that $\beta > 0$, the stability condition is satisfied iff $\alpha/\beta < 1$.

MLE procedure. Consistency, asymptotic normality and efficiency of the MLE, for a univariate Exponential Hawkes process, are provided in Ogata (1978) and Clinet and Yoshida (2017). The expression for $\log \mathcal{L}$ in this model is reported below. To perform MLE we construct and use a Matlab code, which is available upon request, employing the package fmincon for the function $-\log \mathcal{L}$ of the parameters describing the model jump intensity.
Before applying the minimization to the empirical data we assessed the quality of the MLE estimators through a simulation study. To simulate the paths of a Hawkes process, we fol-

[1] In fact the risk neutral rate r is assumed to be constant, the state price density $\xi_t = e^{-rt} L_t$ is assumed of the form $e^{a_t + b_t X_t}$, with deterministic functions a and b, where $L_t = E[L|\mathcal{F}_t]$ is the conditional expectation of the probability density $L = \frac{dQ}{dP}$. In particular $\lambda^Q = \lambda^P \Phi$, where $\Phi - 1$ is the integrand in the compensated jump measure within the martingale representation of L. From the dynamics of X it turns out that $\log(\Phi(t,x)) = b_t x$, and since λ^P is assumed to be affine then necessarily $b_t \equiv 0$, and then λ^P is a constant.

low Rasmussen (2011), which is based on the Ogata modified thinning algorithm in Ogata (1981). We repeated the MLE on hundreds of simulated paths generated with the same parameters and letting the starting point of the fmincon procedure vary. Then we repeated with many different parameter choices. The estimation results obtained with horizon time length $T = 19$ years show that the number of observations we dispose of allows us to identify the true parameters [2]. The starting points for the fmincon procedure where taken either randomly or coinciding with the parameter triplet of the simulated process, or close to it.

QQ-plot.

Any point process N with strictly positive λ such that $\int_0^{+\infty} \lambda_s ds = +\infty$, is transformed in a simple Poisson process with parameter 1, whose law is denoted $PP(1)$, through the time change $\Lambda_t = \int_0^t \lambda_s ds$ (Bowsher, 2007, Thm 4.1). More precisely, N is such that $\{N_{\Lambda_t}\}_{t\geq 0} \sim PP(1)$, where $\sim$ denotes equality in distribution, and thus *the transformed time duration between 2 jumps* (*transformed duration*), given by $\Lambda_{T_j} - \Lambda_{T_{j-1}} = \int_{T_{j-1}}^{T_j} \lambda_t dt$, are independent random variables with law $\mathcal{E}(1)$,, i.e., the exponential law with parameter one. Therefore, we design the QQ-plot, which compares the quantiles of the record of values $\int_{\hat{T}_{j-1}}^{\hat{T}_j} \hat{\lambda}_t dt$ obtained with the model with the quantiles of a record of $\hat{N}_T$ independent values assumed by an $\mathcal{E}(1)$ random variable.
For a candidate model N to be reasonable, it must at least to be that the QQ-plot is close to the bisector line of the Carthesian plane. The QQ-plots displayed for the 20 selected assets are shown in Figure 1.4.3.

Expression of the likelihood of the Hawkes process

The density of the law of a Hawkes process N on $[0, T]$ with respect to the Lebesgue measure m on $\mathbb{R}_+$ is given by (Daley and Vere-Jones, 2008, Proposition 7.3.III)

$$\log \mathcal{L} = -\int_0^T \lambda_t dt + \int_0^T \log(\lambda_t) dN_t.$$

Denote the antiderivative of $\Phi(x)$ by $\tilde{\Phi}(x)$, and note that, by Fubini theorem, we have

$$-\int_0^T \lambda_t dt = -\lambda_0 T - \int_0^T \int_0^t \Phi(t-s) dN_s dt.$$

Conditionally on having observed the times of the jumps occurred within $[0, T]$, the last display equals

$$-\lambda_0 T - \int_0^T \int_s^T \Phi(t-s) dt \; dN_s$$

$$= -\lambda_0 T - \int_0^T [\tilde{\Phi}(T-s) - \tilde{\Phi}(0)] dN_s = -\lambda_0 T - \sum_{\ell: T_\ell < T} (\tilde{\Phi}(T - T_\ell) - \tilde{\Phi}(0)).$$

[2] We also repeated the estimation with alternative Matlab routines: we implement the recursive procedure described in Chen (2016) and also a procedure written and kindly provided by G. Bormetti and F. Lillo of the University of Bologna, still based on the mentioned recursive procedure (see Rambaldi et al., 2015 for details). The results obtained form these procedures are quite the same.

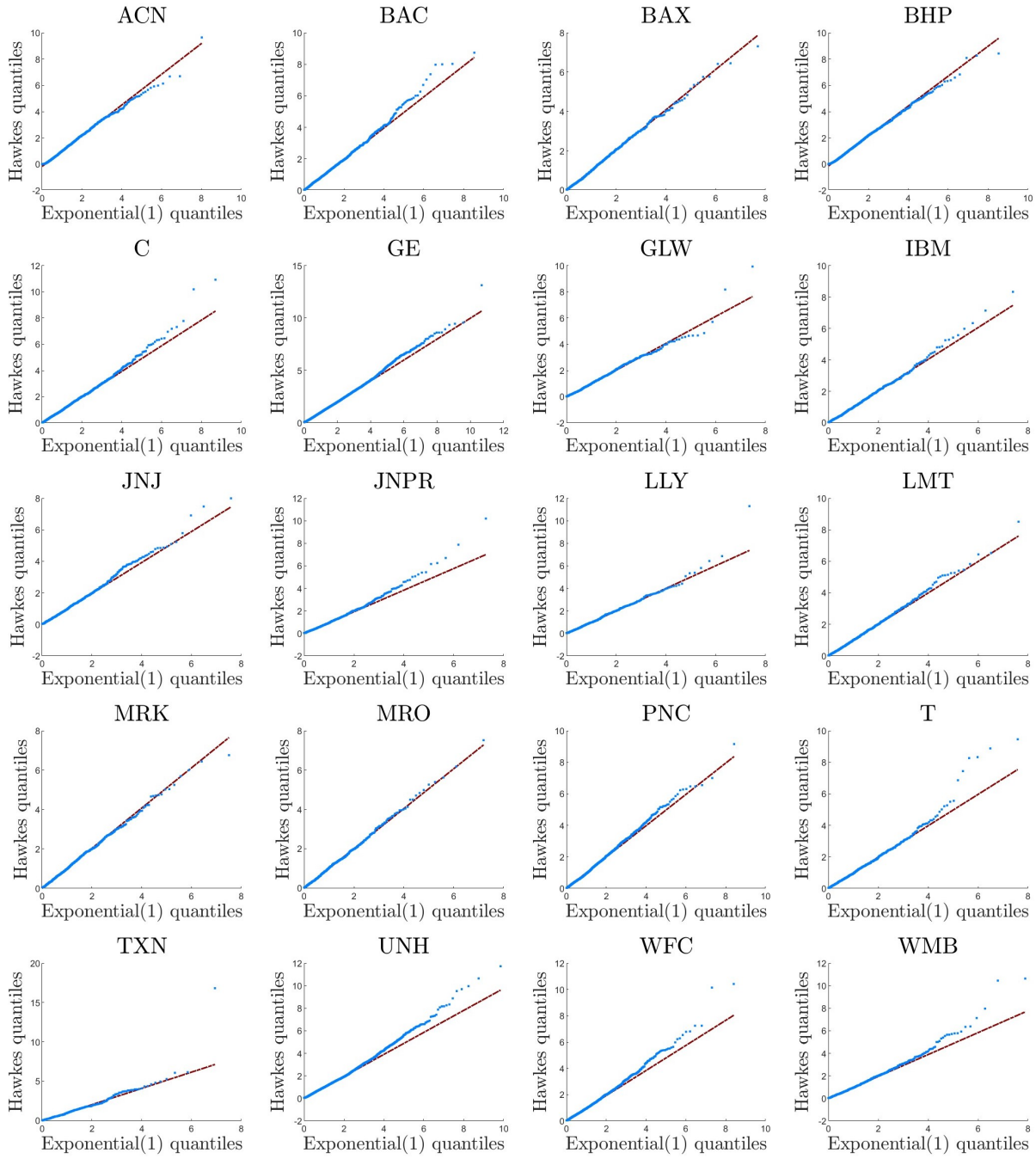

Figure 1: QQ-plot of the empirical law of the estimated jump interarrival times against the law of an exponential random variable with unit parameter, for all assets considered in the analysis.

Furthermore,

$$\int_0^T \log(\lambda_t) dN_t = \sum_{T_\ell < T} \log(\lambda_{T_\ell})$$

$$= \sum_{T_\ell < T} \log\Big(\lambda_0 + \int_0^{T_\ell} \Phi(T_\ell - s) dN_s\Big) = \sum_{T_\ell < T} \log\Big(\lambda 0 + \sum_{T_m < T_\ell} \Phi(T_\ell - T_m)\Big).$$

then

$$\log \mathcal{L} = -\lambda_0 T - \sum_{\ell : T_\ell < T} \Big[\tilde{\Phi}(T - T_\ell) - \tilde{\Phi}(0) - \log\Big(\lambda_0 + \sum_{T_m < T_\ell} \Phi(T_\ell - T_m)\Big)\Big].$$

In particular, for $\Phi(x) = \alpha e^{-\beta x}$ we have $\tilde{\Phi}(x) = -\frac{\alpha}{\beta} e^{-\beta x}$, so that

$$\tilde{\Phi}(u) - \tilde{\Phi}(0) = \int_0^u \Phi(x) dx = \frac{\alpha}{\beta}(1 - e^{-\beta u}). \qquad \square$$

1.4.4 Reliability check on simulations.

For each path of the log-price X, simulated as described in Sec. 5.2, we estimate the times T_j of the occurred jumps as described in Sec. 5.1 and on the values $\hat{T}_j$ we implement MLE for the parameters of an Exponential Hawkes model. With $\epsilon = 0.01$, for each choice of $\underline{s}$ and $\bar{s}$, as in Table 1 below, we compare the theoretical quantities

$$P \doteq P\{T_{i+k} < \bar{s} + t_\epsilon(\bar{s})\}, \quad LB \doteq P\{T_{i+k} < \bar{s} + \underline{t}_\epsilon | N_{\bar{s}} - N_{\underline{s}} = k, \lambda_{\underline{s}}\},$$

$$UB \doteq P\{T_{i+k} < \bar{s} + \bar{t}_\epsilon | N_{\bar{s}} - N_{\underline{s}} = k, \lambda_{\underline{s}}\},$$

given in (5), (8) and (9), with the estimates $\hat{P}, \hat{LB}, \hat{UB}$ obtained using

$$\hat{k} = \hat{N}_{\bar{s}} - \hat{N}_{\underline{s}} \text{ and } \hat{\lambda}_t = \hat{\lambda}_0 + \hat{\alpha} \sum_{\hat{T}_\ell < t} e^{-\hat{\beta}(t - \hat{T}_\ell)}, \text{ for } t = \underline{s}, \bar{s}.$$

We only consider the simulated paths of X for which: $\bar{s}$ does not coincide with a jump time nor with an estimated jump time and the inequality $\lambda_{\bar{s}} > \lambda_0(1 + \epsilon)$ is respected. The latter inequality guarantees that $P \in (0, 1)$, $UB \in [0, 1]$ and $LB \in [0, 1]$.
We repeat for 500 simulated paths of X and report the following average percentage estimation errors, where

'E' stands for average 'relative error' among the different paths;
'$mean(\sigma_{t_i})$' stands for 'average value of spot σ_t among the different time instants $t_i \in [0, T]$';
'$d(a, b)$' stands for average 'relative distance between a and b';
'$hLBlessP$' (resp. '$PlesshUB$') counts the number of paths for which in fact $\hat{LB} \leq P$ (resp. $P \leq \hat{UB}$) is satisfied, as it should be:

$$E^{Mean(\sigma)} = E\left[\frac{|mean(\hat{\sigma}_{t_i}) - mean(\sigma_{t_i})|}{mean(\sigma_{t_i})}\right], \quad E^{N_T} = E\left[\frac{|\hat{N}_T - N_T|}{N_T}\right],$$

$$E^{\lambda_0} = E\left[\frac{|\hat{\lambda}_0 - \lambda_0|}{\lambda_0}\right], \quad E^{\alpha} = E\left[\frac{|\hat{\alpha} - \alpha|}{\alpha}\right], \quad E^{\beta} = E\left[\frac{|\hat{\beta} - \beta|}{\beta}\right],$$

$$d(P,\hat{LB}) = E\left[\frac{P-\hat{LB}}{P}\right], \quad d(P,\hat{UB}) = E\left[\frac{\hat{UB}-P}{P}\right],$$
$$hLBlessP = E\left[\mathbf{1}_{\{\hat{LB}<P\}}\right] \quad PlesshUB = E\left[\mathbf{1}_{\{P<\hat{UB}\}}\right].$$

We find on average 1.5 (with std 1.7) spurious jumps and we are not able to identify on average 425 (with std 46.5) true jumps out of an average number of jumps equal to $T \cdot E[N_1] = n\delta \cdot \frac{\lambda_0\beta}{\beta-\alpha} \approx 1121$. Few couples of jumps fall within the same 5-minute interval and are identified as a single jump, while most unidentified jumps happen to fall below the threshold.
The average relative estimation errors are reported below, in Table 1.

Table 1: Average percentage estimation errors $E^{Mean(\sigma)}, E^{N_T}, E^{\lambda_0}, E^{\alpha}, E^{\beta}, d(P,\hat{LB}), d(P,\hat{UB})$ on 500 simulated paths of a process X following the dynamics described in (21). Standard errors are within brackets. We further report the average values of: $LB, \hat{LB}, P, \hat{P}, UB, \hat{UB}$; number k of true jumps within $[\underline{s}, \bar{s})$ and number $\hat{k}$ of the estimated jumps; $hLBlessP$ and $PlesshUB$.

Spot σ and point process N		
$E^{Mean(\sigma)}$= 0.16492 (0.01867)	E^{N_T}= 0.38122 (0.033264)	
E^{λ_0}=0.22515 (0.072138),	E^{α}= 0.31392 (0.088472)	E^{β}=0.19648 (0.094791)
$\underline{s}$ = 0.18, $\bar{s}$ = 0.215		
k= 2.2403 (2.7241),	$\hat{k}$= 1.3539 (1.8568)	
LB= 0.74327 (0.17464)	P= 0.79736 (0.20572)	UB= 0.83601 (0.22505)
$\hat{LB}$=0.72766 (0.17148)	$\hat{P}$=0.76713 (0.19415)	$\hat{UB}$= 0.79874 (0.21351)
$d(P,\hat{LB})$=0.20355 (0.51262)	$d(P,\hat{UB})$= 0.17005 (0.51825)	
hLBlessP= 0.76299,	PlesshUB= 0.63636	
$\underline{s}_2$ = 0.02, $\bar{s}_2$ = 0.07		
k= 3.4643 (2.9505)	$\hat{k}$= 2.1591 (1.7491)	
LB= 0.73475 (0.072081)	P=0.87912 (0.10661)	UB= 0.9541 (0.097762)
$\hat{LB}$= 0.73362 (0.093001)	$\hat{P}$= 0.84499 (0.1104)	$\hat{UB}$= 0.92181 (0.11042)
$d(P,\hat{LB})$=0.17885 (0.099701)	$d(P,\hat{UB})$= 0.090136 (0.10321)	
hLBlessP= 0.91234	PlesshUB= 0.79221	

2 List of all assets considered in the empirical analysis

Table 2: List of all assets considered: Name, Ticker, Sector, Sample period.

Name	Ticker	Sector	Sample period
ALCOA	AA	Aluminum	30/4/07-10/3/22
APPLE	AAPL	Personal Computers	2/1/03-8/3/22
ABBOTT LABORATORIES	ABT	Drug Manufacturers - Major	2/1/03-15/6/06
ACCENTURE PLC	ACN	Information Technology Services	2/1/03-8/3/22
APPLIED MATERIALS	AMAT	Semiconductor Equipment & Materials	2/1/03-8/3/22
AMGEN	AMGN	Biotechnology	2/1/03-8/3/22
ALPHA NATURAL RESOURCES	ANR	Industrial Metals & Minerals	16/2/05-15/7/15
APACHE CORP.	APA	Independent Oil & Gas	2/1/03-8/3/22
ANADARKO PETROLEUM CORPORATION	APC	Independent Oil & Gas	2/1/03-2/8/19
AMERICAN EXPRESS COMPANY	AXP	Credit Services	2/1/03-8/3/22
BOEING CO.	BA	Aerospace/Defense Products & Services	2/1/03-8/3/22
BANK OF AMERICA CORPORATION	BAC	Regional - Mid-Atlantic Banks	2/1/03-8/3/22
BAXTER INTERNATIONAL	BAX	Medical Instruments & Supplies	2/1/03-8/3/22
BAKER HUGHES INCORPORATED	BHI	Oil & Gas Equipment & Services	2/1/03-30/6/17
BHP BILLITON LTD.	BHP	Industrial Metals & Minerals	3/1/03-8/3/22
BAIDU	BIDU	Internet Information Providers	8/8/05-8/3/22
THE BANK OF NEW YORK MELLON CORPORATION	BK	Asset Management	2/1/03-8/3/22
BRISTOL-MYERS SQUIBB COMPANY	BMY	Drug Manufacturers - Major	2/1/03-8/3/22
BP PLC	BP	Major Integrated Oil & Gas	2/1/03-8/3/22
BROADCOM CORP.	BRCM	Semiconductor - Integrated Circuits	2/1/03-29/1/16
PEABODY ENERGY CORP.	BTU	Industrial Metals & Minerals	4/4/17-8/3/22
CITIGROUP	C	Money Center Banks	2/1/03-8/3/22
CATERPILLAR	CAT	Farm & Construction Machinery	2/1/03-8/3/22
CF INDUSTRIES HOLDINGS	CF	Agricultural Chemicals	12/8/05-8/3/22
CHESAPEAKE ENERGY CORPORATION	CHK	Independent Oil & Gas	11/2/21-8/3/22
CLIFFS NATURAL RESOURCES	CLF	Steel & Iron	3/1/03-8/3/22
CUMMINS	CMI	Diversified Machinery	10/12/03-8/3/22
CAPITAL ONE FINANCIAL CORP.	COF	Credit Services	2/1/03-8/3/22
CONOCOPHILLIPS	COP	Major Integrated Oil & Gas	2/1/03-8/3/22
SALESFORCE.COM	CRM	Application Software	24/6/04-8/3/22
CISCO SYSTEMS	CSCO	Networking & Communication Devices	2/1/03-8/3/22
CENTURYLINK,	CTL	Telecom Services - Domestic	2/1/03-17/9/20
CHEVRON CORPORATION	CVX	Major Integrated Oil & Gas	2/1/03-8/3/22
E. I. DU PONT DE NEMOURS AND COMPANY	DD	Chemicals - Major Diversified	28/5/19-8/3/22
DEERE & COMPANY	DE	Farm & Construction Machinery	2/1/03-8/3/22
DELL	DELL	Personal Computers	27/12/18-8/3/22
THE DOW CHEMICAL COMPANY	DOW	Chemicals - Major Diversified	21/3/19-8/3/22
DEVON ENERGY CORPORATION	DVN	Independent Oil & Gas	12/10/04-8/3/22
EMC CORPORATION	EMC	Data Storage Devices	2/1/03-6/9/16
EMERSON ELECTRIC CO.	EMR	Industrial Equipment & Components	2/1/03-8/3/22
EOG RESOURCES	EOG	Independent Oil & Gas	2/1/03-8/3/22
EL PASO CORP.	EP	Oil & Gas Pipelines	2/1/03-24/5/12
EXPRESS SCRIPTS	ESRX	Health Care Plans	2/1/03-20/12/18
FREEPORT-MCMORAN COPPER & GOLD	FCX	Copper	2/1/03-8/3/22
GENERAL ELECTRIC COMPANY	GE	Diversified Machinery	2/1/03-10/3/22
GOLDCORP	GG	Gold	3/1/03-17/4/19
GILEAD SCIENCES	GILD	Biotechnology	2/1/03-9/3/22
CORNING	GLW	Diversified Electronics	2/1/03-8/3/22

Table 2: List of all assets considered: Name, Ticker, Sector, Sample period (continued).

Name	Ticker	Sector	Sample period
GOOGLE	GOOG	Internet Information Providers	28/3/14-9/3/22
THE GOLDMAN SACHS GROUP,	GS	Diversified Investments	2/1/03-9/3/22
HALLIBURTON COMPANY	HAL	Oil & Gas Equipment & Services	2/1/03-9/3/22
HESS CORPORATION	HES	Oil & Gas Refining & Marketing	13/3/07-9/3/22
HONEYWELL INTERNATIONAL	HON	Aerospace/Defense Products & Services	2/1/03-9/3/22
HEWLETT-PACKARD COMPANY	HPQ	Diversified Computer Systems	2/1/03-10/3/22
INTERNATIONAL BUSINESS MACHINES CORP.	IBM	Diversified Computer Systems	2/1/03-9/3/22
INTEL CORPORATION	INTC	Semiconductor - Broad Line	2/1/03-9/3/22
ITAU UNIBANCO HOLDING S.A.	ITUB	Foreign Money Center Banks	20/5/09-9/3/22
JOHNSON & JOHNSON	JNJ	Drug Manufacturers - Major	2/1/03-10/3/22
JUNIPER NETWORKS	JNPR	Networking & Communication Devices	2/1/03-10/3/22
JPMORGAN CHASE & CO.	JPM	Money Center Banks	3/1/03-10/3/22
ELI LILLY & CO.	LLY	Drug Manufacturers - Major	2/1/03-10/3/22
LOCKHEED MARTIN CORPORATION	LMT	Aerospace/Defense Products & Services	2/1/03-10/3/22
LYONDELLBASELL INDUSTRIES NV	LYB	Specialty Chemicals	14/10/10-10/3/22
MEDTRONIC	MDT	Medical Appliances & Equipment	2/1/03-10/3/22
METLIFE	MET	Life Insurance	2/1/03-10/3/22
THE MOSAIC COMPANY	MOS	Specialty Chemicals	25/10/04-10/3/22
MERCK & CO.	MRK	Drug Manufacturers - Major	2/1/03-10/3/22
MARATHON OIL CORPORATION	MRO	Oil & Gas Refining & Marketing	3/1/03-10/3/22
MORGAN STANLEY	MS	Investment Brokerage - National	17/1/06-10/3/22
MICROSOFT CORPORATION	MSFT	Application Software	2/1/03-10/3/22
MICRON TECHNOLOGY	MU	Semiconductor- Memory Chips	2/1/03-10/3/22
NEWMONT MINING CORP.	NEM	Gold	3/1/03-10/3/22
NATIONAL OILWELL VARCO,	NOV	Oil & Gas Equipment & Services	16/3/05-10/3/22
NETAPP	NTAP	Data Storage Devices	2/1/03-10/3/22
NVIDIA CORPORATION	NVDA	Semiconductor - Specialized	2/1/03-10/3/22
ORACLE CORPORATION	ORCL	Application Software	2/1/03-10/3/22
OCCIDENTAL PETROLEUM CORPORATION	OXY	Major Integrated Oil & Gas	2/1/03-10/3/22
PFIZER	PFE	Drug Manufacturers - Major	2/1/03-10/3/22
PNC FINANCIAL SERVICES GROUP	PNC	Money Center Banks	2/1/03-10/3/22
PRUDENTIAL FINANCIAL,	PRU	Life Insurance	2/1/03-10/3/22
QUALCOMM INCORPORATED	QCOM	Communication Equipment	2/1/03-10/3/22
TRANSOCEAN LTD.	RIG	Oil & Gas Drilling & Exploration	2/1/03-10/3/22
RIO TINTO PLC	RIO	Industrial Metals & Minerals	11/2/10-10/3/22
SCHLUMBERGER LIMITED	SLB	Oil & Gas Equipment & Services	2/1/03-10/3/22
SANDISK CORP.	SNDK	Semiconductor- Memory Chips	2/1/03-11/5/16
SIMON PROPERTY GROUP	SPG	REIT - Retail	3/1/03-10/3/22
AT&T	T	Telecom Services - Domestic	2/1/03-10/3/22
TEVA PHARMACEUTICAL INDUSTRIES LIMITED	TEVA	Drug Manufacturers - Other	2/1/03-10/3/22
TEXAS INSTRUMENTS	TXN	Semiconductor - Broad Line	2/1/03-10/3/22
UNITEDHEALTH GROUP	UNH	Health Care Plans	2/1/03-10/3/22
U.S. BANCORP	USB	Regional - Midwest Banks	3/1/03-10/3/22
VALE S.A.	VALE	Industrial Metals & Minerals	4/5/09-10/3/22
VALERO ENERGY CORPORATION	VLO	Oil & Gas Refining & Marketing	2/1/03-10/3/22
VERIZON COMMUNICATIONS	VZ	Telecom Services - Domestic	2/1/03-10/3/22
WELLS FARGO & COMPANY	WFC	Money Center Banks	2/1/03-10/3/22
WILLIAMS COMPANIES	WMB	Oil & Gas Pipelines	2/1/03-10/3/22

References

Aït-Sahalia, Y., J. Cacho-Diaz, and R. J. Laeven (2015). 'Modeling financial contagion using mutually exciting jump processes'. *Journal of Financial Economics Vol. 117*, pp. 585–606.

Bollerslev, T. and V. Todorov (2011). Tails, fears, and risk premia. *The Journal of Finance 66(6)*, 2165–2211.

Bowsher, C. G. (2007). 'Modelling security market events in continuous time: Intensity based, multivariate point process models'. *Journal of Econometrics Vol. 141*, pp. 876–912.

Chen, Y. (2016). 'Likelihood Function for Multivariate Hawkes Processes'. *Preprint (5 pages) available on https://www.math.fsu.edu/ ychen/research/HawkesLikelihood.pdf*.

Clinet, S. and N. Yoshida (2017). 'Statistical inference for ergodic point processes and application to Limit Order Book'. *Stochastic Processes and their Applications Vol. 127*, pp. 1800–1839.

Daley, D. J. and D. Vere-Jones (2008). *An introduction to the theory of point processes. Vol. II: General theory and structure.* (2nd revised and extended ed.). New York, NY: Springer.

Duffie, D., J. Pan, and K. Singleton (2000). 'Transform analysis and asset pricing for affine jump-diffusions'. *Econometrica Vol. 68*, pp. 1343–1376.

Figueroa-López, J. E. and C. Mancini (2019). 'Optimum thresholding using mean and conditional mean squared error'. *Journal of Econometrics Vol. 208*, pp. 179–210.

Ogata, Y. (1978). 'The asymptotic behaviour of maximum likelihood estimators for stationary point processes'. *Ann. Inst. Stat. Math. Vol. 30*, pp. 243–261.

Ogata, Y. (1981). 'On Lewis Simulation Method for Point Processes'. *IEEE Transactions on Information Theory Vol. IT-27*, pp. 23–31.

Rambaldi, M., P. Pennesi, and F. Lillo (2015). Modeling foreign exchange market activity around macroeconomic news: Hawkes-process approach. *Physical Review E 91(1)*, 012819.

Rasmussen, J. (2011). 'Lecture Notes: Temporal Point Processes and the Conditional Intensity Function'. *http://arxiv.org/abs/1806.00221*.

Zhuang, J., Y. Ogata, and D. Vere-Jones (2002). 'Stochastic declustering of space-time earthquake occurrences'. *J. Am. Stat. Assoc. Vol. 97*, pp. 369–380.